Journal of Molecular Graphics and Modelling 28 (2010) 891–898

Contents lists available at ScienceDirect

Journal of Molecular Graphics and Modelling

journal homepage: www.elsevier.com/locate/JMGM

Structural stability and electronic property of $C_{68}X_4$ (X = H, F, and Cl) fullerene compounds

Shu-Wei Tang, Jing-Dong Feng, Li-Li Sun, Feng-Di Wang, Hao Sun, Ying-Fei Chang*, Rong-Shun Wang*

Institute of Functional Material Chemistry, Faculty of Chemistry, Northeast Normal University, Changchun, Jilin 130024, People's Republic of China

ARTICLE INFO

Article history:
Received 4 September 2009
Received in revised form 13 March 2010
Accepted 29 March 2010
Available online 3 April 2010

Keywords:
Density functional theory (DFT)
Isolated pentagon rule (IPR)
$C_{68}X_4$
Stability
Electronic property

ABSTRACT

A systematic study on the geometrical structures and electronic properties of $C_{68}X_4$ (X = H, F, and Cl) fullerene compounds has been carried out on the basis of density functional theory. In all classical $C_{68}X_4$ isomers with two adjacent pentagons and one quasifullerene isomer [C_s:C_{68}(f)] containing a heptagon in the framework, the C_s:0064 isomers are most favorable in energy. The addition reaction energies of $C_{68}X_4$ (C_s:0064) are high exothermic, and $C_{68}F_4$ is more thermodynamically accessible. The $C_{68}X_4$ (C_s:0064) possess strong aromatic character, with nucleus independent chemical shifts ranging from −22.0 to −26.1 ppm. Further investigations on electronic properties indicate that $C_{68}F_4$ and $C_{68}Cl_4$ could be excellent electron-acceptors for potential photonic/photovoltaic applications in consequence of their large vertical electron affinities (3.29 and 3.15 eV, respectively). The Mulliken charge populations and partial density of states are also calculated, which show that decorating C_{68} fullerene with various X atoms will cause remarkably different charge distributions in $C_{68}X_4$ (C_s:0064) and affect their electronic properties distinctly. Finally, the infrared spectra of the most stable $C_{68}X_4$ (C_s:0064) molecules are simulated to assist further experimental characterization.

1. Introduction

Since the discovery of C_{60} [1], along with subsequent purifying in macroscopic quantities [2], fullerenes and their derivatives, as novel materials for electrochemical catalysis, hydrogen storage media, antiviral agents, superconductors, and optical devices, have attracted a great deal of attention [3–8]. The conventional fullerenes (C_n, n = 60 and ≥70) synthesized so far faithfully satisfy the well-known empirical isolated pentagon rule (IPR) [9], which rules out those carbon cages containing adjacent pentagons. Therefore, non-IPR fullerenes are predicted to be neither stable in structures nor isolable in experiments due to the high steric strains and the resonance destabilization pertaining to the adjacent pentagons. However, these non-IPR fullerenes, in the range of C_{52}–C_{58} and C_{62}–C_{68}, show intensive signals in mass spectra [10,11].

Thanks to the rapid development of flexible and precise experiment techniques, the recent experimental attempts have achieved significant evidence for non-IPR fullerenes and their derivatives. The fullerenes, ranging from C_{62} to C_{68}, have been synthesized successfully in the form of metallofullerenes. The electron transfer between the inner metal atoms (trimetallic nitride) and the external cages release much local strains originating from the fused pentagons, and result in high chemical stabilities and special properties of these metallofullerenes. Examples comprise such stable metallofullerenes $Sc_2@C_{66}$ [12], $Sc_2C_2@C_{68}$ [13], and $A_xSc_{3-x}N@C_{68}$ (x = 0–2) [14,15]. Paralleling the intensive achievements on synthesis and characterizations of non-IPR metallofullerenes, some hydrides and halides have also been isolated gradually. The chlorine derivatives of C_{50}–C_{64} have been synthesized by Xie et al. [16,17] in the modified graphite arc-discharge process, and the exact structures of $C_{50}Cl_{10}$ [17–19], $C_{56}Cl_{10}$ [20,21], and $C_{64}Cl_4$ [17,22] have been determined unambiguously with a wide range of experimental methods and density functional theory (DFT) calculations. In 2005, Troshin et al. [23] have nicely synthesized milligram quantities of two stable heptagon-containing derivatives $C_{58}F_{18}$ and $C_{58}F_{17}CF_3$ through fluorinating C_{60} at 550 °C. More recently, a new hydride $C_{64}H_4$ [24], with four hydrogen atoms attaching to the vertexes of a triplet of directly fused pentagons, has been successfully prepared by incorporating methane in the fullerene productions. These encouraging discoveries related to non-IPR fullerenes give promising ways to stabilize non-IPR fullerenes, and enrich the bank of stable fullerene derivatives for practical applications in the future.

Among multitudinous non-IPR fullerenes, C_{68} is a particularly promising target for experimental synthesis. As a C_2-unit was added to the C_{68} fullerene, C_{70} can be generated, so C_{68} may be one of precursors to C_{70}. Moreover, the successful isolations of

* Corresponding authors. Tel.: +86 431 8509 9511; fax: +86 431 8509 9511.
E-mail addresses: changyf299@nenu.edu.cn (Y.-F. Chang), wangrs@nenu.edu.cn (R.-S. Wang).

1093-3263/$ – see front matter © 2010 Elsevier Inc. All rights reserved.
doi:10.1016/j.jmgm.2010.03.009

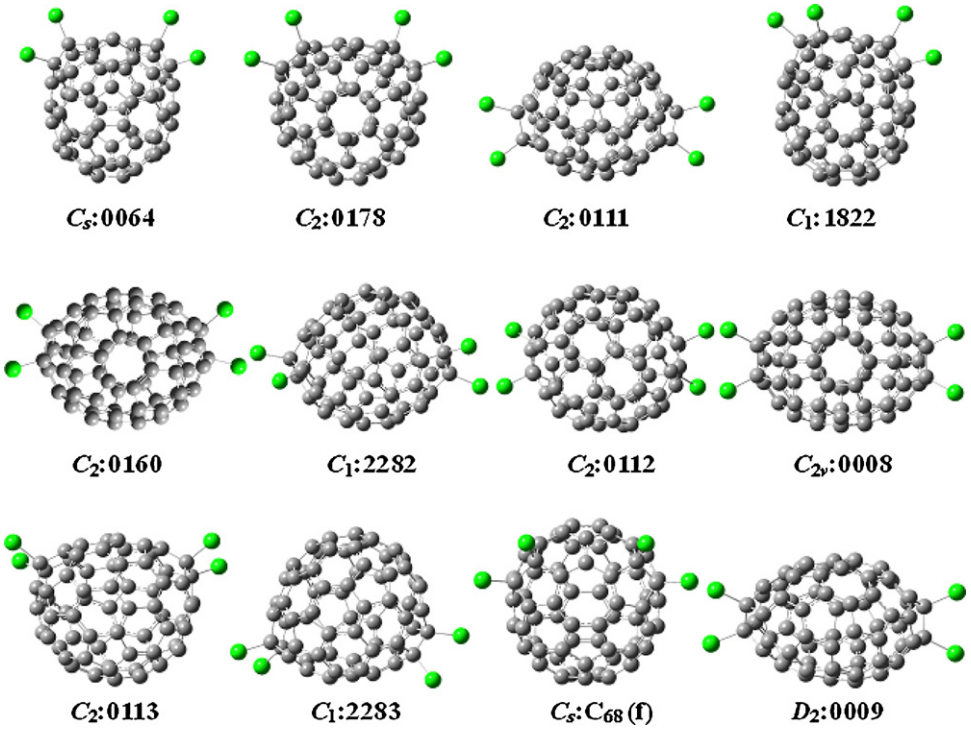

Fig. 1. Schematic structures of twelve $C_{68}X_4$ (X = H, F and Cl) isomers.

$Sc_2C_2@C_{68}$ (C_{2v}) [13] and $Sc_3N@C_{68}$ (D_3) [14] indicate that the endohedral chemical modification of different metallic clusters at the adjacent pentagons could obtain diversiform symmetry metallofullerenes. Consequently, like other famous non-IPR fullerene derivatives [such as $C_{50}Cl_{10}$, $C_{56}Cl_{10}$, and $C_{64}X_4$ (X = H and Cl)], we expect that C_{68} could be stabilized through hydrogenation and halogenation on the fused pentagon–pentagon vertexes. In present work, a comprehensive investigation on structural stabilities, and electronic properties of $C_{68}X_4$ (X = H, F, and Cl) fullerene derivatives on the basis of DFT is performed. Our present study would gain an insight into properly understanding the stabilization of non-IPR fullerenes, and could also motivate further experimental efforts on $C_{68}X_4$ (X = H, F, and Cl) compounds.

2. Computational details

Using spiral algorithm [25], all the 6332 classical isomers (the cages are only composed of pentagons and hexagons) of C_{68} fullerene are generated by means of FULLGEN program [26], and sorted in terms of the numbers of adjacency pentagons. According to the pentagon adjacency penalty rule (PAPR) [27], the most stable structure is that showing the least number of adjacent pentagons. The adjacent pentagon fusions are usually the most active sites in fullerene frameworks, and chemical modification on the fused vertexes of adjacent pentagons can release large steric stains. On the basis of all eleven classical isomers having the lowest number of two adjacent pentagons in the complete set of C_{68} and one stable heptagon-containing isomer proposed by Chen et al. [28] through removal of a C_2-unit from D_{5h} C_{70} fullerene, we have introduced four X (X = H, F, and Cl) atoms into all the pentagon–pentagon fusion vertexes of these fullerene isomers to generate $C_{68}X_4$ compounds.

Geometry and frequency calculations of $C_{68}X_4$ (X = H, F, and Cl) were performed with BLYP (Becke exchange functional in conjunction with Lee–Yang–Parr correlation functional) method within generalized gradient approximation (GGA) [29,30]. The basis sets consist of the double numerical atomic orbitals augmented by diffusion functions (DND) and polarization functions (DNP), comparable to Gaussian 6-31G(d) and 6-31G(d, p) sets. The BLYP/DND and BLYP/DNP methods are chosen because of their good performance in fullerenes [31] and nanotubes [32] calculations, and the structural parameters are in excellent agreement with experimental results. Geometry optimizations are conducted with convergence criterion of 5×10^{-3} a.u. on the maximum force and the maximum displacement, and 5×10^{-5} a.u. on the total energy. These computations are of all-electron type and carried out using the DMol^3 computer software [33]. The aromaticity of $C_{68}X_4$ (X = H, F, and Cl) is evaluated by the nucleus independent chemical shift (NICS) [34,35], which is calculated at the molecule center utilizing gauge-independent atomic orbital (GIAO) method [36]. The hybrid B3LYP functional (formed by combining Becke's three parameter nonlocal hybrid exchange functional [37] and the nonlocal correlation functional of Lee–Yang–Parr, [29]) in combination with 6-311G(d, p) basis set within GAUSSIAN 03 package [38] are used to compute the NICS values of $C_{68}X_4$ compounds, and the accuracy and efficiency of this theoretical method have been verified by many previous calculations. [39,40] To measure the strain relaxation of $C_{68}X_4$ (X = H, F, and Cl) derivatives caused by additional reactions, the pyramidalization angle (θ_p) [41,42] is calculated using the π-orbital axis vector approach (POAV) as implemented in the Mol2Mol program [43].

3. Results and discussions

3.1. Relative energies and structures of $C_{68}X_4$ (X = H, F, and Cl)

The molecular structures of all $C_{68}X_4$ (X = H, F, and Cl) isomers optimized by means of BLYP/DND method are displayed in Fig. 1, and the corresponding relative energies and lowest vibration frequencies obtained at the same level are presented in Table 1. For comparison purpose, in the parentheses of Table 1, the corresponding relative energies of these compounds computed at BLYP/DNP//BLYP/DND level are also listed. The labels of eleven

Table 1
Relative energies (E_{rel}, kcal/mol), HOMO–LUMO energy gaps (E_{gap}, eV) and the lowest vibration frequencies (γ, cm^{-1}) of $C_{68}X_4$ (X = H, F, and Cl) isomers predicted at BLYP/DND level. The values of E_{rel} in parenthesis are obtained by means of BLYP/DNP//BLYP/DND method.

Isomer	$C_{68}H_4$			$C_{68}F_4$			$C_{68}Cl_4$		
	E_{rel}	E_{gap}	γ	E_{rel}	E_{gap}	γ	E_{rel}	E_{gap}	γ
C_s:0064	0.00 (0.00)	0.13	205.86	0.00 (0.00)	0.16	177.18	0.00 (0.00)	0.15	101.61
C_2:0178	5.46 (6.60)	0.65	212.50	7.87 (7.88)	0.61	171.05	8.92 (8.09)	0.23	101.15
C_2:0111	6.00 (7.46)	0.62	205.16	10.72 (10.64)	0.50	172.15	12.82 (10.65)	0.53	99.16
C_1:1822	7.18 (7.17)	0.49	204.98	8.25 (8.26)	0.44	171.98	8.00 (8.81)	0.44	100.23
C_2:0160	11.62 (14.29)	0.43	201.44	15.27 (15.28)	0.44	168.44	15.29 (16.18)	0.37	98.99
C_1:2282	12.27 (19.32)	0.16	205.35	19.19 (19.20)	0.15	171.48	22.26 (20.09)	0.12	99.72
C_2:0112	13.46 (20.52)	0.13	205.61	14.40 (21.15)	0.15	178.67	17.16 (21.90)	0.14	102.64
C_{2v}:0008	13.85 (18.87)	0.32	197.62	17.01 (23.42)	0.29	173.25	24.15 (21.96)	0.31	106.72
C_2:0113	18.14 (22.59)	0.27	208.31	25.26 (25.28)	0.18	178.85	21.79 (25.04)	0.21	100.45
C_1:2283	22.40 (24.42)	0.55	206.47	27.10 (27.11)	0.47	176.01	29.31 (20.09)	0.10	102.13
C_s:C_{68}(f)	33.79 (33.79)	0.08	216.86	34.06 (34.05)	0.11	159.31	36.62 (34.46)	0.12	96.54
D_2:0009	34.92 (36.57)	0.62	202.42	35.25 (35.25)	0.63	171.30	37.88 (37.74)	0.58	101.61

classical $C_{68}X_4$ isomers (simply denoted as C_s:0064, C_2:0178, and C_2:0111, etc.) derive from the number indices of the corresponding fullerene isomers generated by FULLGEN program [26], which follow the order of appearance in spiral nomenclature and combine with diversely molecular symmetries. The non-classical isomer C_s:C_{68}(f) with one heptagon in the framework is defined in terms of the work of Chen et al. [28]. As can be seen from Table 1, by attaching four H atoms to the fused vertexes of two adjacent pentagons, C_s:0064 isomer is predicted to have the lowest energy, and followed up by C_2:0178 and C_2:0111 isomers, with 5.46 and 6.00 kcal/mol higher in relative energy at the BLYP/DND level. The C_s:C_{68}(f) isomer having a heptagon in the cage framework is less stable relative to C_s:0064, which has a large relative energy of 33.79 kcal/mol. The relative energies of $C_{68}H_4$ system predicted by means of BLYP/DNP//BLYP/DND method agree well with those of computing at BLYP/DND level in principle, although the order of a few isomers varies. The C_2:0112 isomer possesses the largest deviation of 7.06 kcal/mol calculated with above two theoretical methods. The fluorination and chlorination at the pentagon–pentagon fusion vertexes of C_{68} isomers show similar effect to hydrogenation. As a result, the cage subunits in the $C_{68}X_4$ molecules with the same addition patterns have almost the same shapes except for the only difference that the C–F and C–Cl bonds are much longer than C–H bonds. After decoration of F and Cl atoms on C_{68} isomers, the orders of stability for $C_{68}F_4$ and $C_{68}Cl_4$ systems changed with respect to those of $C_{68}H_4$ compounds. However, the orders of relative energies in $C_{68}X_4$ (X = F and Cl) still keep the whole tendency as those of H addition. The $C_{68}F_4$ (C_s:0064) and $C_{68}Cl_4$ (C_s:0064) are also predicted to be the most stable isomers at the BLYP/DND level, and the other isomers are at least 7.87 and 8.00 kcal/mol higher. The orders of relative energies for $C_{68}F_4$ and $C_{68}Cl_4$ systems predicted at BLYP/DNP//BLYP/DND level are in good accord with the results obtained at BLYP/DND level, with the largest differences of 6.75 and 9.22 kcal/mol for $C_{68}F_4$ (C_2:0112) and $C_{68}Cl_4$ (C_1:2283), respectively. At the same time, the $C_{68}F_4$ [C_s:C_{68}(f)] and $C_{68}Cl_4$ [C_s:C_{68}(f)] also show large relative energies, similar to the case of $C_{68}H_4$ [C_s:C_{68}(f)]. Hence, we can conclude that the X (X = H, F and Cl) addition on the non-classical isomers of C_{68} are inaccessible in energy.

Previous experimental and theoretical studies [44,45] show that the structural information of a molecule can be accessed in an indirect way through vibration frequency, i.e., the frequency of normal vibration modes can indicate whether the structure is a global minimum with all positive frequency, or a transition state with one negative frequency, or a higher order stationary point with more than one negative frequency. As presented in Table 1, the lowest vibration frequencies for all $C_{68}X_4$ (X = H, F, and Cl) molecules are positive values, confirming that these structures are the real global minima on the potential energy hypersurface. Moreover, the lowest vibration frequencies for $C_{68}X_4$ molecules with the same addition patterns decrease with the order of $C_{60}Cl_{18} < C_{60}F_{18} < C_{60}H_{18}$.

The energy gaps (E_{gap}) between the highest occupied and the lowest unoccupied molecular orbitals (HOMO and LUMO) for twelve $C_{68}X_4$ (X = H, F, and Cl) molecules predicted at BLYP/DND level are also presented in Table 1. The E_{gap}s of $C_{68}X_4$ are very small, much smaller than those of $C_{50}X_{10}$ and $C_{58}X_{18}$ calculated at B3LYP/6-31G(d) level [18,19,46]. The E_{gap}s for the most stable $C_{68}X_4$ (C_s:0064) are 0.13, 0.16 and 0.15 eV, respectively. However, it should be noted that the E_{gap}s do not necessarily correlate with the relative stabilities of $C_{68}X_4$ compounds. For instance, the $C_{68}H_4$ (C_2:0178), $C_{68}F_4$ (D_2:0009) and $C_{68}Cl_4$ (D_2:0009) possess the largest E_{gap}s of 0.65, 0.63 and 0.58 eV, respectively, but they are less stable with respect to C_s:0064 isomers. Therefore, in the following discussions, we will focus our study on the geometrical structures and electronic properties of $C_{68}X_4$ (C_s:0064) molecules.

The sketch structure of $C_{68}X_4$ (C_s:0064) is presented in Fig. 1, and the corresponding Schlegel diagram is shown in Fig. 2, in which all carbons are numbered consecutively to distinguish the distinct C–C bonds. The cage subunit in $C_{68}X_4$ (C_s:0064) shows a close resemblance to D_{5h} C_{70} fullerene, except for only one difference that the tapering top in $C_{68}X_4$ (C_s:0064) is composed of a triplet of directly fused hexagons. Neighboring the fused hexagons, there is a pair of adjacent pentagons, where considerable local strains can be expected. To confirm the accuracy of BLYP/DND method, we have optimized the I_h C_{60} and compared the bond lengths with experiment values. Our calculations show that the C–C bond lengths are in reasonable agreement (average differences smaller than 0.01 Å) with experimental nuclear magnetic resonance (NMR) and X-ray data for C_{60} [47,48], indicating a high reliability of BLYP/DND method. The C(sp^2)–C(sp^2), C(sp^2)–C(sp^3), and C(sp^3)-C(sp^3) bond lengths of $C_{68}X_4$ (C_s:0064) obtained by BLYP/DND method are listed in Table S1 (available in Supplementary Material). By the comparison of C–C bond lengths in $C_{68}X_4$ molecules, we found that the C(sp^2)–C(sp^3) and C(sp^3)–C(sp^3) bond lengths elongate significantly in consequence of the sp^2 to sp^3 hybridization, whereas the other C(sp^2)–C(sp^2) bonds are almost unaffected. Consequently, the cage subunits in $C_{68}X_4$ molecules show nearly the same geometries, and the largest deviations of C(sp^2)–C(sp^2), C(sp^2)–C(sp^3) and C(sp^3)–C(sp^3) bonds are 0.004, 0.018 and 0.023 Å, respectively. In general, the C(sp^2)–C(sp^3) bonds of $C_{68}X_4$ compounds are longer than the C(sp^2)–C(sp^2) bonds, but substantially shorter than those of type C(sp^3)–C(sp^3). Take $C_{68}Cl_4$ for example, the average bond lengths of C(sp^2)–C(sp^2), C(sp^2)–C(sp^3) and C(sp^3)–C(sp^3) are 1.435, 1.506 and 1.602 Å, respectively, which are comparable to the corresponding C–C bonds of D_{5h} $C_{50}Cl_{10}$ (1.426, 1.526 and 1.604 Å, respectively) [18,19]. The C–X (X = H, F, and Cl) bond lengths at four

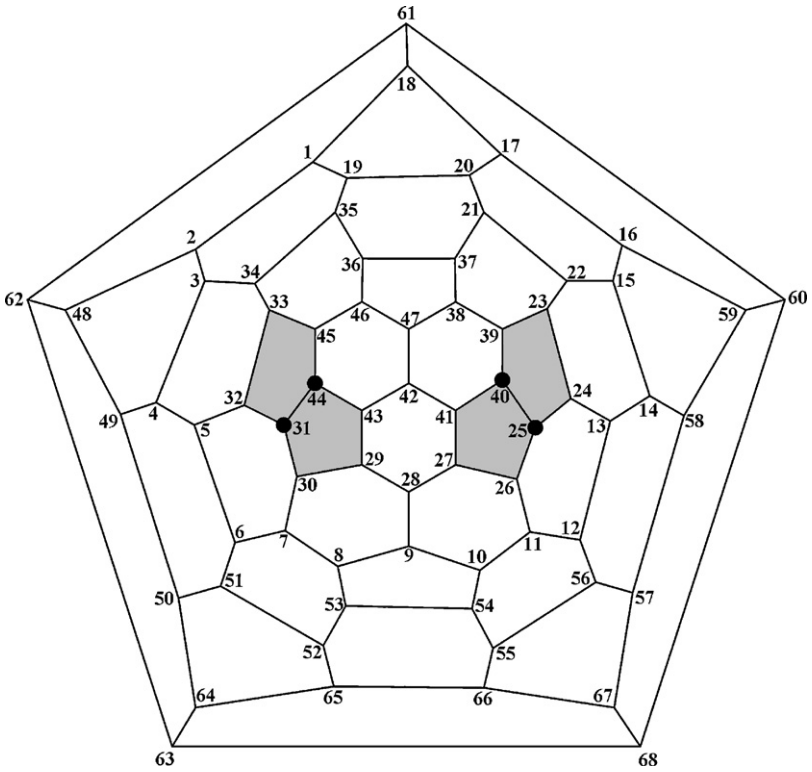

Fig. 2. Schlegel diagram for $C_{68}X_4$ (C_s:0064), in which all pentagons are highlighted with grey color and X (X = H, F and Cl) atoms are indicated by black dots.

carbon sites of $C_{68}X_4$ molecules are presented in Table S2 (as provided in Supplementary Material), and the average C–H, C–F, and C–Cl bond lengths are 1.103, 1.416 and 1.843 Å, respectively. The average C–X bond lengths are in good agreement with those predictions in compounds of $C_{58}X_{18}$ (X = H, F, and Cl) [46] and $C_{66}X_4$ (X = H, F, and Cl) [49] reported recently.

The local strain energy in nonplanar conjugated molecules, such as fullerenes and nanotubes, is the main driving force for chemical reactivity. By analyzing a great number of nonplanar conjugated organic molecules, Haddon [41,42] has found that the local strain energy could be expressed in terms of θ_p, which was defined by the angle between the π-orbital and adjacent σ-bonds, minus $\pi/2$ radian. Like other non-IPR fullerenes, significant strains can be expected at the fusion sites of adjacent pentagons in C_{68} fullerene. Owing to the hydrogenation and halogenation are mainly occurred at the pentagon–pentagon fusion sites [such as $C_{50}Cl_{10}$, $C_{56}Cl_{10}$, and $C_{64}X_4$ (X = H and Cl)], we only show the θ_ps at high strain carbon sites, i.e., those carbons pertaining to the two abutting pentagons. The values of θ_p for C_{68} and $C_{68}X_4$ derivatives based on POAV analysis are presented in the Table S3 (as shown in Supplementary Material). In the case of C_{68}, the curvatures in the fused pentagon areas are obviously higher than those in the other regions. The θ_ps at pentagon–pentagon fusion vertexes are 0.2630 radian (15.07°) for C(25) and C(31), 0.2827 radian (16.20°) for C(40) and C(44) (see Fig. 2), comparable to that of D_{5h} C_{50} (15.5°), and significantly larger than that of C_{60} (11.6°). Accordingly, these carbons have potential inclination to combine with X (X = H, F, and Cl) atoms and change to sp^3 hybridization to release the local strains. In $C_{68}X_4$, the reacting sites [C(25), C(31), C(40), and C(44)] of two adjacent pentagons become saturated by X (X = H, F, and Cl) atoms and the local strains in these areas release effectively. Moreover, the values of θ_p for those carbons near the pentagon–pentagon fusions are also much smaller than the counterparts of C_{68} fullerene.

In addition to expatiating on the influence stemming from the addition of X atoms on the structural changes of two adjacent pentagons, the θ_ps of the rest of carbons also change slightly after the addition reaction. Haddon has suggested that the local strains could be measured with the parameter $\sum\theta_p^2$, and the quantities of strain relaxation are actually equal to the $\sum(\Delta\theta_p^2)$, which are the difference of the $\sum\theta_p^2$ between C_{68} and $C_{68}X_4$ molecules, as listed in Table 2. For instance, the $\sum\theta_p^2$ of C_{68} is 2.57671, and the $\sum\theta_p^2$, $\sum(\Delta\theta_p^2)$ of $C_{68}H_4$ are 2.10634 and 0.47037, respectively, which indicate that the strain energy release 18.3% during the process of H addition. However, it must be noted that the strain energy relaxation is one of the major factors that determine the reactivity of the fullerenes and their derivatives, and it does not correlate with the relative stabilities of $C_{68}X_4$ molecules.

3.2. Aromatic character of $C_{68}X_4$

The NICS proposed by Schleyer et al. [34,35] demonstrated to be a useful criterion for measuring aromaticity of a molecule. The computed NICS value in the center of molecule has essentially the same value as the ^{3}He NMR chemical shift, which is a valuable experimental tool for charactering fullerenes and their derivatives [50,51], and can be reproduced computationally reasonably well [52]. Consequently, the calculated NICS value has been employed to

Table 2
The HOMO and LUMO energies (eV), vertical electron affinities (VEA, eV), vertical ionization potentials (VIP, eV), NICS values (ppm), $\sum\theta_p^2$ and $\sum(\Delta\theta_p^2)$[a] for C_{68} and $C_{68}X_4$ (X = H, F and Cl). All of the predictions are performed using BLYP/DND method except for the NICS calculated at B3LYP/6-311G(d, p) level.

Molecule	E_{HOMO}	E_{LUMO}	VEA	VIP	NICS	$\sum\theta_p^2$	$\sum(\Delta\theta_p^2)$
C_{68}	−4.72	−3.45	3.06	6.36	27.6	2.57671	
$C_{68}H_4$	−4.13	−4.00	2.49	5.74	−22.0	2.10634	0.47037
$C_{68}F_4$	−4.95	−4.79	3.29	6.53	−25.9	2.08722	0.48949
$C_{68}Cl_4$	−4.82	−4.67	3.15	6.46	−26.1	2.11292	0.46379

[a] $\sum(\Delta\theta_p^2) = \sum\theta_p^2(C_{68}) - \sum\theta_p^2(C_{68}X_4)$.

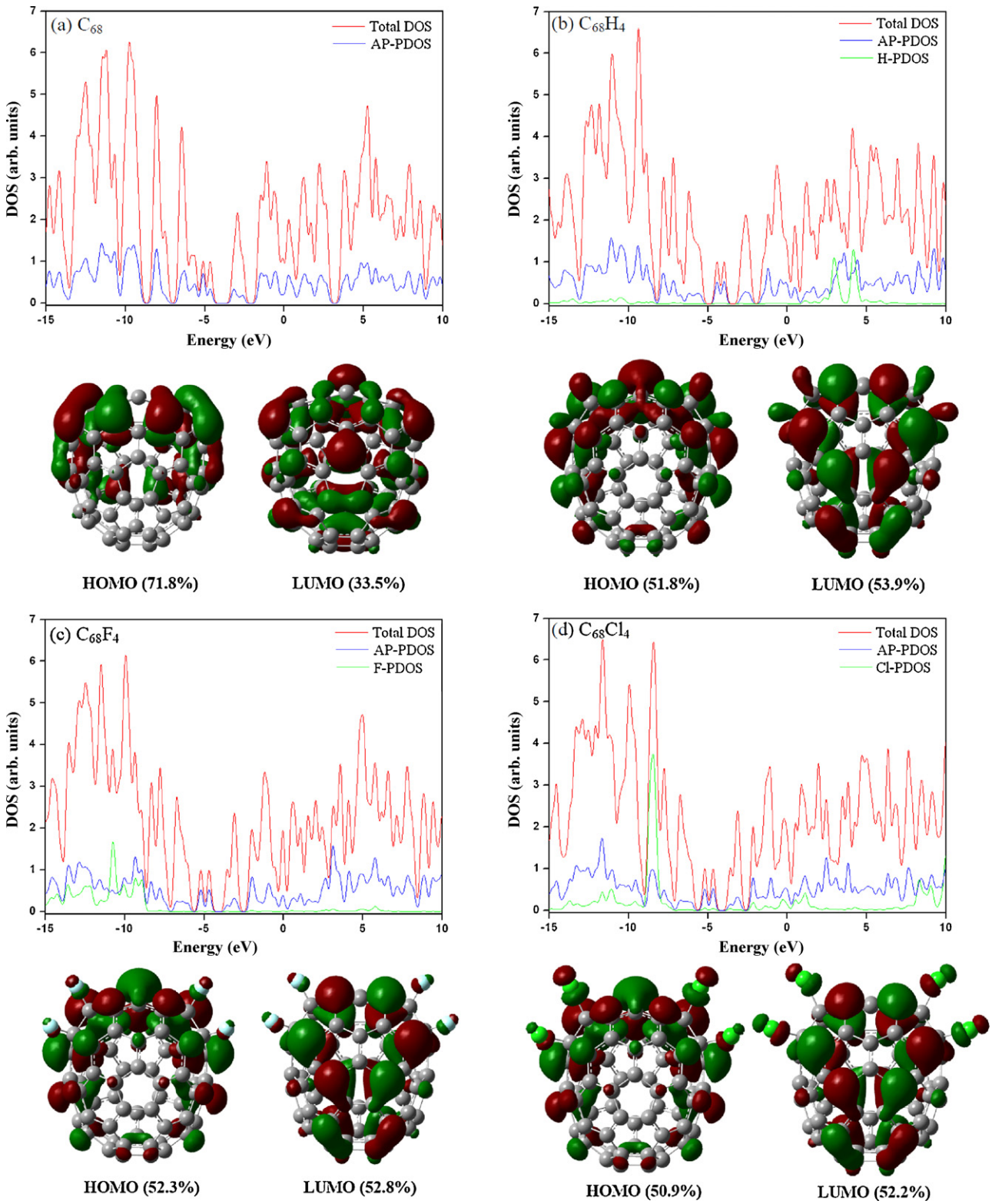

Fig. 3. Total density of states (total DOS), partial density of states (PDOS), and frontier molecular orbitals (FMO) obtained by B3LYP/6-31G(d) method of C_{68} and $C_{68}X_4$ (X = H, F and Cl). The values in parentheses of the FMOs represent the contributions of carbons belonging to the two adjacent pentagons (AP) in the framework of C_{68} fullerene.

characterize aromaticity of fullerenes instead of ^{3}He NMR. According to the NICS definition, aromaticity and antiaromaticity are characterized by negative and positive NICS values, respectively, and nonaromaticity by a value close to zero. The NICS values of C_{68} and $C_{68}X_4$ (C_s:0064) calculated using GIAO B3LYP/6-311G(d, p) method on the basis of the geometries optimized at BLYP/DND level are summarized in Table 2. Evidently, the C_{68} exhibits strong antiaromatic character, as evidenced by a remarkably positive NICS value (27.6 ppm), comparable to the prediction of Chen et al. [28]. However, after the X (X = H, F, and Cl) attaching on the fused pentagon–pentagon vertexes, charge transfer takes place between the X atoms and cage subunit. As a consequence, $C_{68}X_4$ molecules

are high aromatic, and the aromaticity increased with the order of $C_{68}H_4 < C_{68}F_4 < C_{68}Cl_4$ in principle. The NICS values for $C_{68}H_4$, $C_{68}F_4$ and $C_{68}Cl_4$ are −22.0, −25.9 and −26.1 ppm, respectively. Compared with the decachlorofullerene D_{5h} $C_{50}Cl_{10}$ [−17.5 ppm calculated at the B3LYP/6-31G(d) level] [18], $C_{68}X_4$ possess more negative NICS values, indicating the better delocalization of electron densities.

3.3. Electronic properties of $C_{68}X_4$

To gain an insight into the electronic properties of $C_{68}X_4$ (C_s:0064) (X = H, F, and Cl) derivatives, the energies of HOMO and LUMO, vertical electron affinity (VEA, energy difference between the neutral and mono-anionic molecules on the basis of the same neutral geometry), and vertical ionization potential (VIP, energy difference between the mono-cationic and the neutral molecule based on the same neutral geometry) are performed at BLYP/DND level, and the calculated results are presented in Table 2. The eigenvalues of HOMO and LUMO for C_{68} are −4.72 and −3.45 eV, respectively, very close to those of D_{5h} C_{50} (−4.24 and −3.77 eV, respectively) [53]. The VEA of C_{68} is 3.06 eV, much larger than those of C_{60} and C_{70} (EA = 2.67 and 2.68 eV, obtained by the electron photo-detachment method) [54]. The additions of hydrogen and halogen at the pentagon–pentagon fusions of C_{68} have significant difference in frontier molecular orbitals (FMO). Compared with C_{68}, the E_{HOMO} of $C_{68}H_4$ lifts by about 0.6 eV, while the E_{LUMO} reduces to −4.00 eV, which results in a small E_{gap} of 0.13 eV. The VEA and VIP of $C_{68}H_4$ are 2.49 and 5.74 eV, respectively, 0.57 and 0.62 eV smaller than those of C_{68}. However, the E_{HOMO} and E_{LUMO} of $C_{68}X_4$ (X = F and Cl) significantly shift down relative to those of C_{68}, especially for the E_{LUMO} levels. The VEA of $C_{68}F_4$ and $C_{68}Cl_4$ are 3.29 and 3.15 eV, larger than those of C_{68} by 0.23 and 0.09 eV; while the VIP are 6.53 and 6.46 eV, respectively, 0.17 and 0.10 eV higher than those of C_{68}. It is well known that halofullerenes, e.g., $C_{60}X_n$ (X = F and Cl), can serve as excellent electron-acceptors with potential photonic/photovoltaic applications. As their analogues, similar application could be expected for $C_{68}F_4$ and $C_{68}Cl_4$.

We also perform Mulliken charge analysis for $C_{68}X_4$ and present the atomic charge of C(sp^3) at the pentagon–pentagon vertexes and X atoms in Table S2. The additions of X (X = H, F, and Cl) atoms to C_{68} fullerene change the charge populations of carbons. By analysis of atomic charge in $C_{68}X_4$ (C_s:0064), we found that the added X atoms mainly affect the charges of C(sp^3) atoms and the influence on other carbons is negligible. As three different types of substituent groups fused to C_{68}, the charge transfers between X atoms and carbon cage are quite different. For $C_{68}H_4$, the Mulliken atomic charges of C(sp^3) and H atoms range from −0.268 to −0.273 *e* and 0.158 to 0.159 *e*, respectively. For electron transfers, the C(sp^3) atoms at the pentagon–pentagon vertexes are electron-acceptors, and H atoms are electron donors. The addition of F leads to a significantly different behavior on C_{68} fullerene. Since F are good electron withdrawing groups, the C(sp^3) atoms connected with F atoms in $C_{68}F_4$ possess positive charge (range from 0.180 to 0.188 *e*); and F atoms are negative charged with −0.346 and −0.348 *e*, which are comparable with those of $C_{60}F_{18}$ [46] [the natural atomic charge for F atoms of $C_{60}F_{18}$ calculated at the B3LYP/6-31G(d, p) level are in the range of −0.33 to −0.35 *e*], suggesting an inverse electron transfer. As a different structure with $C_{68}F_4$, the atomic charges of C(sp^3) atoms are negative in $C_{68}Cl_4$ [−0.125 *e* for C(25) and C(31), −0.123 *e* for C(40) and C(44), respectively], and the Cl atoms possess slightly negative charges (range from −0.090 to −0.095 *e*), similar to the natural bond orbital calculations for $C_{58}Cl_{18}$ molecules [46]. In conclusion, a proper chemical modification on the pentagon–pentagon fusions of non-IPR fullerenes could change the electronic structures significantly, and adding different substituting group will bring different consequences.

The electronic density of states (DOS) and partial density of states (PDOS) can provide a convenient comprehensive view of the electronic structures and orbital populations of clusters and solids. Fig. 3 shows the total DOS, PDOS of adjacent pentagons (AP-PDOS) and the added X (X = H, F, and Cl) atoms (X-PDOS), as well as FMOs obtained by B3LYP/6-31G(d) method of C_{68} and $C_{68}X_4$ compounds. As the AP-PDOS shows, the carbon orbitals of the two adjacent pentagons have significant contributions to total DOS of C_{68} and $C_{68}X_4$ compounds. For C_{68}, the HOMO is bonding molecular orbital (π) which contains a mass of *p* orbital ingredients, and the LUMO is antibonding orbital in principle. Natural bond orbital (NBO) [55–57] analysis shows that the carbons of adjacent pentagons have much larger coefficients than the others in the C_{68} cage. Quantifying localization degree in the frame of Mulliken population analysis (MPA) for the contributions from these carbons of adjacent pentagons, we have 71.8% for the HOMO and 33.5% for the LUMO. As a consequence, these regions possess high chemical activity and should be the more favored sites for further addition reaction. In $C_{68}X_4$ molecules, both HOMOs and LUMOs are antibonding orbitals, and the electronic structures are very similar except for a slight difference in the extent of localization for added X (X = H, F, and Cl) atoms. The contributions from X atoms to FMOs of $C_{68}X_4$ are very small that can be neglected (1.8% and 2.1% for HOMO and LUMO of $C_{68}H_4$, 1.6% and 2.0% for HOMO and LUMO of $C_{68}F_4$, and 4.5% and 5.1% for HOMO and LUMO of $C_{68}Cl_4$). After the addition of hydrogen and halogen at the adjacent pentagon fusions of C_{68}, the contributions from the carbons belonging to adjacent pentagons to HOMOs decrease sharply (51.8, 52.3, and 50.9% for the HOMOs of $C_{68}H_4$, $C_{68}F_4$, and $C_{68}Cl_4$, respectively). Meanwhile, the corresponding values for the LUMOs are 53.9% in $C_{68}H_4$, 52.8% in $C_{68}F_4$, and 52.2% in $C_{68}Cl_4$, larger than those of C_{68}. Such phenomenon indicates that after the passivation of X atoms at the pentagon–pentagon fusion vertexes, the other carbons with large electron density in adjacent pentagons still possess high steric strains, and should be active sites for further addition reactions. This scenario can be seen clearly from the graphical plots, where green and red colors represent the positive and negative wavefunctions, respectively.

3.4. Reactive energy of addition reaction

Binding two X_2 to the pentagon–pentagon fusions of C_{68} release much strain energies of C_{68}, and the reaction energy (E_r) of hydrogenation, fluorination, and chlorination is defined as Eq. (1). Eq. (2) is used to calculate the E_rs of $C_{68}X_4$ (X = H, F, and Cl) compounds to measure their thermodynamic stabilities, in which E_r, $E(C_{68}X_4)$, $E(C_{68})$, and $E(X_2)$ stand for the reaction energy, total energies of $C_{68}X_4$, C_{68}, and X_2 (X = H, F, and Cl) respectively. Normally, the E_r is negative number, and the larger negative number denotes greater stability.

$$C_{68} + 2X_2 \rightarrow C_{68}X_4 \quad (1)$$

$$E_r = E(C_{68}X_4) - E(C_{68}) - 2E(X_2) \quad (2)$$

The addition reactions of $C_{68} + 2X_2 \rightarrow C_{68}X_4$ (X = H, F, and Cl) are exothermic with negative values of E_rs (−32.72 kcal/mol for per H_2, −111.79 kcal/mol for per F_2 and −35.59 kcal/mol for per Cl_2), comparable to the reaction energies (per H_2, F_2 and Cl_2) of $C_{58}X_{18}$ molecules [46], indicating that $C_{68}H_4$, $C_{68}F_4$ and $C_{68}Cl_4$ are favorable in energy. However, compared with the hydrogenation, fluorination, and chlorination reaction energies (per H_2, F_2 and Cl_2) of D_{5h} $C_{50}X_{10}$ (−50.9, −131.8 and −50.6 kcal/mol for $C_{50}H_{10}$, $C_{50}F_{10}$ and $C_{50}Cl_{10}$, respectively) [18,19], the reaction energies of $C_{68}X_4$ are smaller. Such a variation may be attributed to the fact that in $C_{50}X_{10}$, ten X atoms are added to five pentagon–pentagon fusion vertexes and release much local strain energies of C_{50} cage, whereas

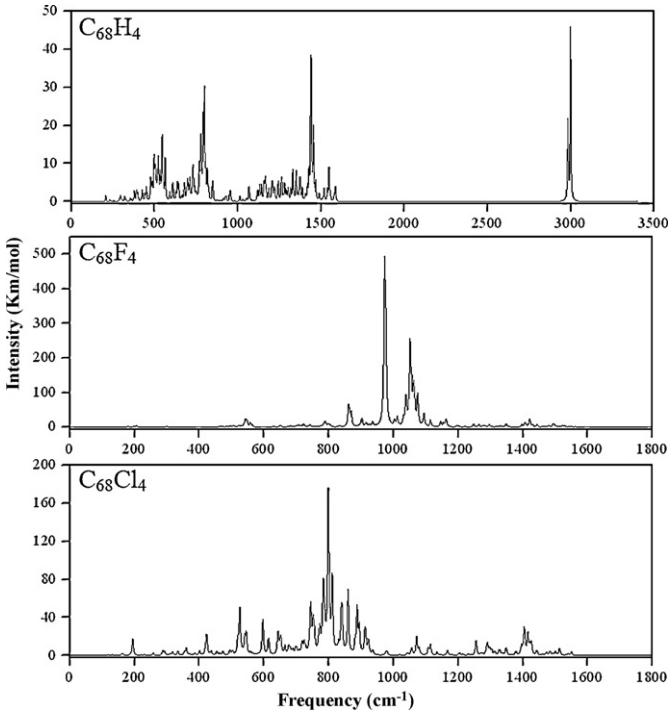

Fig. 4. Simulated IR spectra of $C_{68}X_4$ (X = H, F and Cl).

only four X atoms are added to the fusions of adjacent pentagons in $C_{68}X_4$.

3.5. Infrared spectra

In order to provide a verifying basis for the experimental identification, we investigate the IR spectra of $C_{68}X_4$ (C_s:0064) (X = H, F, and Cl) at the BLYP/DND level. As Fig. 4 shows, the IR spectra of all the $C_{68}X_4$ molecules can be roughly divided into three major regions: the first one (from 200 to 950 cm^{-1}) mainly corresponds to breathing modes of the cages, the second one (from 1000 to 1600 cm^{-1}) corresponds to the C–C stretching modes, and the third one corresponds to the C–X stretching modes. The major regions of C–H, C–F, and C–Cl stretching modes are located in the range of 2950–3100, 950–1020, and 750–910 cm^{-1}, respectively. For $C_{68}H_4$, there is a sharp peak with intensity of 33.2 km/mol at 2999 cm^{-1}, which corresponds to C(40 and 44)–H stretching modes (see notation in Fig. 2). However, the IR spectra of $C_{68}F_4$ and $C_{68}Cl_4$ are quite different from that of $C_{68}H_4$, which only extend to the frequency about 1600 cm^{-1} and without obvious separation regions. Moreover, $C_{68}F_4$ and $C_{68}Cl_4$ lack a clear region of C–X stretching modes in IR spectra. The reasons may be that H atom is much lighter relative to C atom, resulting in a high peak appears far from that of carbons at high frequency regions. By contrast, F and Cl atoms are heavier than C atoms, so the C–F and C–Cl vibration modes strongly couple with C–C vibration modes, which lead to IR spectra of $C_{68}F_4$ and $C_{68}Cl_4$ could not be parted into different regions. At the same time, the intensities of C–X (X = F and Cl) stretching modes are significantly stronger than those of C–C vibration modes. The $C_{68}F_4$ possesses the most intense peak of 443.1 km/mol at 972 cm^{-1}, while the highest peak of $C_{68}Cl_4$ is 171.8 km/mol at 799 cm^{-1}, all of them are mainly corresponding to the stretching modes C(40 and 44)–X bonds. In summary, the IR spectra of $C_{68}X_4$ (X = H, F, and Cl) vary with the addition of different X atoms, which may be helpful for future experimental characterization.

4. Conclusions

A systematic calculation on the basis of DFT has been performed on the structural stabilities and electronic properties of non-IPR $C_{68}X_4$ (X = H, F and Cl) fullerene compounds. Among all geometric structures of $C_{68}X_4$, C_s:0064 isomers are the most energetically favorable. The combinations of four X atoms at the pentagon–pentagon fusion vertexes release much local strain energies of C_{68} fullerene. The NICS research shows that $C_{68}X_4$ (C_s:0064) derivatives possess strong aromatic character, with the NICS values ranging from −22.0 to −26.1 ppm. The $C_{68}F_4$ and $C_{68}Cl_4$ should be good electron-acceptors in consequence of their large VEA values (3.29 and 3.15 eV, respectively). The PDOS analysis suggests that $C_{68}X_4$ derivatives can be stabilized by decreasing the contributions of carbons belonging to the two adjacent pentagons to the total DOS, and the counterparts from the added X atoms are so small that can be neglected. Finally, the infrared spectra of $C_{68}X_4$ derivatives are simulated to provide helpful information for further experiment identification.

Acknowledgements

Financial supports from the National Natural Science Foundation of China (Project No. 20773021) and the Fundamental Research Funds for the Central Universities (Project No. 09SSXT121) are gratefully acknowledged. The authors appreciate the invaluable comments and good suggestions from the reviewers.

Appendix A. Supplementary data

Supplementary data associated with this article can be found, in the online version, at doi:10.1016/j.jmgm.2010.03.009.

References

[1] H.W. Kroto, J.R. Heath, S.C. O'Brien, R.F. Curl, R.E. Smalley, C_{60}: Buckminsterfullerene, Nature 318 (1985) 162–163.
[2] W. Krätschmer, L.D. Lamb, K. Fostiropoulos, D.R. Huffman, Solid C_{60}: a new form of carbon, Nature 347 (1990) 354–358.
[3] H. Shinohara, Endohedral metallofullerenes, Rep. Prog. Phys. 63 (2000) 843–892.
[4] M.S. Dresselhaus, G. Dresselhaus, P.C. Eklund, Science of Fullerenes and Carbon Nanotubes, Academic, New York, 1996.
[5] K. Holczer, O. Klein, S.M. Huang, R.B. Kaner, K.J. Fu, R.L. Whetten, F. Diederich, Alkali-fulleride superconductors: synthesis, composition, and diamagnetic shielding, Science 252 (1991) 1154–1157.
[6] S. Pekker, A. Jánossy, L. Mihaly, O. Chauvet, M. Carrard, L. Forró, Single-crystalline $(KC_{60})_n$: a conducting linear alkali fulleride polymer, Science 265 (1994) 1077–1078.
[7] R.E. Dinnebier, O. Gunnarsson, H. Brumm, E. Koch, P.W. Stephens, A. Huq, M. Jansen, Structure of haloform intercalated C_{60} and its influence on superconductive properties, Science 296 (2002) 109–113.
[8] W. Mickelson, S. Aloni, W.Q. Han, J. Cumings, A. Zettl, Packing C_{60} in boron nitride nanotubes, Science 300 (2003) 467–469.
[9] H.W. Kroto, The stability of the fullerenes C_n, with n = 24, 28, 32, 36, 50, 60 and 70, Nature 329 (1987) 529–531.
[10] S.C. O'Brien, J.R. Heath, R.F. Curl, R.E. Smalley, Photophysics of buckminsterfullerene and other carbon cluster ions, J. Chem. Phys. 88 (1998) 220–230.
[11] X. Lu, Z.F. Chen, Curved Pi-conjugation, aromaticity, and the related chemistry of small fullerenes (<C_{60}) and single-walled carbon nanotubes, Chem. Rev. 105 (2005) 3643–3696.
[12] C.R. Wang, T. Kai, T. Tomiyama, T. Yoshida, Y. Kobayashi, E. Nishibori, M. Takata, M. Sakata, H. Shinohara, C_{66} fullerene encaging a scandium dimer, Nature 408 (2000) 426–427.
[13] Z.Q. Shi, X. Wu, C.R. Wang, X. Lu, H. Shinohara, Isolation and characterization of Sc_2C_2@C_{68}: a metal-carbide endofullerene with a non-IPR carbon cage, Angew. Chem. Int. Ed. 45 (2006) 2107–2111.
[14] S. Stevenson, P.W. Fowler, T. Heine, J.C. Duchamp, G. Rice, T. Glass, K. Harich, E. Hajdu, R. Bible, H.C. Dorn, A stable non-classical metallofullerene family, Nature 408 (2000) 427–428.
[15] M.M. Olmstead, H.M. Lee, J.C. Duchamp, S. Stevenson, D. Marciu, H.C. Dorn, A.L. Balch, Sc_3N@C_{68}: folded pentalene coordination in an endohedral fullerene that does not obey the isolated pentagon rule, Angew. Chem. Int. Ed. 42 (2003) 900–903.

[16] S.Y. Xie, F. Gao, X. Lu, R.B. Huang, C.R. Wang, X. Zhang, M.L. Liu, S.L. Deng, L.S. Zheng, Capturing the labile fullerene [50] as $C_{50}Cl_{10}$, Science 304 (2004) 699–1699.
[17] X. Han, S.J. Zhou, Y.Z. Tan, X. Wu, F. Gao, Z.J. Liao, R.B. Huang, Y.Q. Feng, X. Lu, S.Y. Xie, L.S. Zheng, Crystal structures of saturn-like $C_{50}Cl_{10}$ and pineapple-shaped $C_{64}Cl_4$: geometric implications of double- and triple-pentagon-fused chlorofullerenes, Angew. Chem. Int. Ed. 47 (2008) 5340–5343.
[18] X. Lu, Z.F. Chen, W. Thiel, P.V.R. Schleyer, R.B. Huang, L.S. Zheng, Properties of fullerene [50] and D_{5h} decachlorofullerene [50]: a computational study, J. Am. Chem. Soc. 126 (2004) 14871–14878.
[19] Y.F. Chang, J.P. Zhang, B. Hong, H. Sun, Z. An, R.S. Wang, D_{5h} $C_{50}X_{10}$: saturn-like fullerene derivatives (X = F, Cl, Br), J. Chem. Phys. 123 (2005) 094305–094308.
[20] Y.Z. Tan, X. Han, X. Wu, Y.Y. Meng, F. Zhu, Z.Z. Qian, Z.J. Liao, M.H. Chen, X. Lu, S.Y. Xie, R.B. Huang, L.S. Zheng, An entrant of smaller fullerene: C_{56} captured by chlorines and aligned in linear chains, J. Am. Chem. Soc. 130 (2008) 15240–15241.
[21] D.L. Chen, W.Q. Tian, J.K. Feng, C.C. Sun, Structures and electronic properties of $C_{56}Cl_8$ and $C_{56}Cl_{10}$ fullerene compounds, Chemphyschem 8 (2007) 2386–2390.
[22] Q.B. Yan, Q.R. Zheng, G. Su, Structures, electronic properties, spectroscopies, hexagonal monolayer phase of a family of unconventional fullerenes $C_{64}X_4$ (X = H, F, Cl, Br), J. Phys. Chem. C 111 (2007) 549–554.
[23] P.A. Troshin, A.G. Avent, A.D. Darwish, N. Martsinovich, A.K. Abdul-Sada, J.M. Street, R. Taylor, Isolation of two seven-membered ring C_{58} fullerene derivatives: $C_{58}F_{17}CF_3$ and $C_{58}F_{18}$, Science 309 (2005) 278–281.
[24] C.R. Wang, Z.Q. Shi, L.J. Wan, X. Lu, L. Dunsch, C.Y. Shu, Y.L. Tang, H. Shinohara, $C_{64}H_4$: production, isolation, and structural characterizations of a stable unconventional fulleride, J. Am. Chem. Soc. 128 (2006) 6605–6610.
[25] P.W. Fowler, D.E. Manolopoulos, An Atlas of Fullerenes, Oxford, Clarendon, 1995.
[26] G. Brinkmamm, A.W.M. Dress, A constructive enumeration of fullerenes, J. Algorithms 23 (1997) 345–358.
[27] E.E.B. Campbell, P.W. Fowler, D. Mitchell, F. Zerbetto, Increasing cost of pentagon adjacency for larger fullerenes, Chem. Phys. Lett. 250 (1996) 544–548.
[28] D.L. Chen, W.Q. Tian, J.K. Feng, C.C. Sun, C_{68} fullerene isomers, anions, and their metallofullerenes: charge-stabilizing different isomers, Chemphyschem 9 (2008) 454–461.
[29] A.D. Becke, A multicenter numerical integration scheme for polyatomic molecules, J. Chem. Phys. 88 (1988) 2547–2553.
[30] C. Lee, W. Yang, R.G. Parr, Development of the Colle–Salvetti correlation-energy formula into a functional of the electron density, Phys. Rev. B 37 (1988) 785–789.
[31] C.M. Tang, K.M. Deng, W.S. Tan, Y.B. Yuan, Y.Z. Liu, H.P. Wu, D.C. Huang, F.L. Hu, J.L. Yang, X. Wang, Influence of a dichlophenyl group on the geometric structure, electronic properties, and static linear polarizability of La@C_{74}, Phys. Rev. A 76 (2007) 013201–013206.
[32] A.F. Jalbout, A.K. Roy, A.D. Leon, I. Jiménez-Fabián, Metallo[Endo]fullerene-SWNT interactions: a theoretical study, J. Mol. Struct. (Theochem) 858 (2008) 39–45.
[33] B. Delley, An all-electron numerical method for solving the local density functional for polyatomic molecules, J. Chem. Phys. 92 (1990) 508–517.
[34] P.V.R. Schleyer, C. Maerker, A. Dransfeld, H. Jiao, N.J.R.V.E. Hommes, Nucleus independent chemical shifts: a simple and efficient aromaticity probe, J. Am. Chem. Soc. 118 (1996) 6317–6318.
[35] Z. Chen, C.S. Wannere, C. Corminboeuf, R. Puchta, P.V.R. Schleyer, Nucleus independent chemical shifts (NICS) as an aromaticity criterion, Chem. Rev. 105 (2005) 3842–3888.
[36] R. Ditchfield, Self-consistent perturbation theory of diamagnetism I. A gauge-invariant LCAO method for N.M.R. chemical shifts, Mol. Phys. 27 (1974) 789–807.
[37] A.D. Becke, Density-functional thermochemistry. III. The role of exact exchange, J. Chem. Phys. 98 (1993) 5648–5652.
[38] M.J. Frisch, G.W. Trucks, H.B. Schlegel, G.E. Scuseria, M.A. Robb, J.R. Cheeseman, J.A. Montgomery Jr., T. Vreven, K.N. Kudin, J.C. Burant, J.M. Millam, S.S. Iyengar, J. Tomasi, V. Barone, B. Mennucci, M. Cossi, G. Scalmani, N. Rega, G.A. Petersson, H. Nakatsuji, M. Hada, M. Ehara, K. Toyota, R. Fukuda, J. Hasegawa, M. Ishida, T. Nakajima, Y. Honda, O. Kitao, H. Nakai, M. Klene, X. Li, J.E. Knox, H.P. Hratchian, J.B. Cross, C. Adamo, J. Jaramillo, R. Gomperts, R.E. Stratmann, O. Yazyev, A.J. Austin, R. Cammi, C. Pomelli, J.W. Ochterski, P.Y. Ayala, K. Morokuma, G.A. Voth, P. Salvador, J.J. Dannenberg, V.G. Zakrzewski, S. Dapprich, A.D. Daniels, M.C. Strain, O. Farkas, D.K. Malick, A.D. Rabuck, K. Raghavachari, J.B. Foresman, J.V. Ortiz, Q. Cui, A.G. Baboul, S. Clifford, J. Cioslowski, B.B. Stefanov, G. Liu, A. Liashenko, P. Piskorz, I. Komaromi, R.L. Martin, D.J. Fox, T. Keith, M.A. Al-Laham, C.Y. Peng, A. Nanyakkara, M. Challacombe, P.M.W. Gill, B. Johnson, W. Chen, M.W. Wong, C. Gonzalez, J.A. Pople, Gaussian 03, Revision C. 02, Gaussian, Inc., Wallingford, CT, 2004.
[39] M.V. Frash, A.C. Hopkinson, D.K. Bohme, Corannulene as a lewis base: computational modeling of protonation and lithium cation binding, J. Am. Chem. Soc. 123 (2001) 6687–6695.
[40] T.M. Krygowski, E. Pindelska, M.K. Cyrański, G. Häfelinger, Planarization of 1,3,5,7-cyclooctatetraene as a result of a partial rehybridization at carbon atoms: an MP2/6-31G* and B3LYP/6-311G** study, Chem. Phys. Lett. 359 (2002) 158–162.
[41] R.C. Haddon, Chemistry of the fullerenes: the manifestation of strain in a class of continuous aromatic molecules, Science 261 (1993) 1545–1550.
[42] R.C. Haddon, Comment on the relationship of the pyramidalization angle at a conjugated carbon atom to the σ bond angles, J. Phys. Chem. A 105 (2001) 4164–4165.
[43] T.E. Gunda, Mol2Mol version 5.6, University of Debrecen, Debrecen, Hungary, 2008.
[44] A.K. Ott, G.A. Rechtsteiner, C. Felix, O. Hampe, M.F. Jarrold, R.P. Van Duyne, Raman spectra and calculated vibration frequencies of size-selected C_{16}, C_{18}, and C_{20} clusters, J. Chem. Phys. 109 (1998) 9652–9655.
[45] C.H. Choi, M. Kertesz, L. Mihaly, Vibration assignment of all 46 fundamentals of C_{60} and C_{60}^{6-}: scaled quantum mechanical results performed in redundant internal coordinates and compared to experiments, J. Phys. Chem. A 104 (2000) 102–112.
[46] D.L. Chen, W.Q. Tian, J.K. Feng, C.C. Sun, Search for more stable $C_{58}X_{18}$ isomers: stabilities and electronic properties of seven-membered ring $C_{58}X_{18}$ fullerene derivatives (X = H, F, and Cl), J. Phys. Chem. B 111 (2007) 5167–5173.
[47] C.S. Yannoni, P.P. Bernier, D.S. Bethune, G. Meijer, J.R. Salem, NMR determination of the bond lengths in C_{60}, J. Am. Chem. Soc. 113 (1991) 3190–3192.
[48] J.M. Hawkins, A. Meyer, T.A. Lewis, S. Loren, F.J. Hollander, Crystal structure of osmylated C_{60}: confirmation of the soccer ball framework, Science 252 (1991) 312–313.
[49] Q.B. Yan, Q.R. Zheng, G. Su, Theoretical study on the structures, properties and spectroscopies of fullerene derivatives $C_{66}X_4$ (X = H, F, Cl), Carbon 45 (2007) 1821–1827.
[50] M. Saunders, R.J. Cross, H.A. Jiménez-Vázquez, R. Shimshi, A. Khong, Noble gas atoms inside fullerenes, Science 271 (1996) 1693–1697.
[51] G.W. Wang, M. Saunders, A. Khong, R.J. Cross, A new method for separating the isomeric C_{84} fullerenes, J. Am. Chem. Soc. 122 (2000) 3216–3217.
[52] M. Bühl, A. Hirsch, Spherical aromaticity of fullerenes, Chem. Rev. 101 (2001) 1153–1183.
[53] Z.J. Xu, W. Zhang, Z.Y. Zhu, J.G. Han, A density functional study of C_{50} passivation, Chem. Phys. 331 (2006) 111–124.
[54] C. Brink, L.H. Anderson, P. Hvelplund, D. Mathur, J.D. Coldstad, Laser photodetachment of C_{60}^- and C_{70}^- ions cooled in a storage ring, Chem. Phys. Lett. 233 (1995) 52–56.
[55] J.E. Carpenter, F. Weinhold, Analysis of the geometry of the hydroxymethyl radical by the "different hybrids for different spins" natural bond orbital procedure, J. Mol. Struct. (Theochem) 169 (1988) 41–62.
[56] A.E. Reed, L.A. Curtiss, F. Weinhold, Intermolecular interactions from a natural bond orbital, donor–acceptor viewpoint, Chem. Rev. 88 (1988) 899–926.
[57] F. Liu, A.F. Jalbout, Structural, electronic, and magnetic properties of heterofullerene $C_{58}Si$ with odd number of atoms and a near planar tetracoordinate Si atom, J. Mol. Graph. Model. 26 (2008) 1327–1332.